CHAPTER 5
SIMULTANEOUS ELECTROSPINNING OF TWO POLYMER SOLUTIONS IN A SIDE-BY-SIDE APPROACH TO PRODUCE BICOMPONENT FIBERS[†]

5.1 Chapter Summary

Bicomponent fibers, in the range of 100 nm to a few microns, of miscible poly(vinylchloride)/segmented polyurethane (PVC/Estane®) and immiscible poly(vinyl chloride)/poly(vinylidienefluoride) (PVC/PVDF) were produced respectively by electrospinning two polymer solutions in a side-by-side approach. For each of the pairs investigated, PVC/Estane® and PVC/PVDF, energy dispersive spectroscopy was utilized to identify the respective components by detecting the signal corresponding to chlorine, oxygen and fluorine from PVC, Estane® and PVDF respectively. The ratio of the peak intensities of Cl to O in PVC/Estane® and Cl to F in PVC/PVDF were found to vary along the length of the fibers. The ratio of the peak intensities corresponding to Cl and O in the miscible PVC/Estane® was calibrated to the actual wt% of Estane®. The strength of this methodology is to effectively electrospun immiscible and miscible polymer pairs to yield submicron bicomponent fibers that are expected to exhibit a combination of properties from each of its constituent components.

5.2 Introduction

As discussed in earlier chapters, electrospinning is a unique process to produce submicron polymeric fibers in the average diameter range of 100 nm-5 μm.[1-4] Fibers produced by this approach have a diameter that is at least one or two orders of magnitude smaller than those produced by conventional fiber production methods like melt or solution spinning.[5] The effects of several process parameters, such as the applied electric field strength, flow rate, concentration, distance between the capillary and the target have been explored in great detail for different polymer materials.[2,6-10]. Primarily, most of the systems that have been investigated have utilized electrospinning from a single polymer solution or melt. Recently, a few systems where blends of polymers (in the same solvent) and blends of polymer solutions (a four component system) have been electrospun. Blends of polyaniline, a conducting polymer, with poly(ethylene oxide), PEO, in

[†] P. Gupta, G. L. Wilkes, *Polymer* **2003**, *44*, 6353-6359.

chloroform were electrospun to produce filaments in the range of 4 – 20 nm[11,12] that were investigated for their magnetic susceptibility behavior. More specifically, PEO was blended with polyaniline to increase the viscosity of the solution to achieve stable electrospinning. In another study, M13 viruses suspended in 1,1,1,3,3,3-hexafluoro-2-propanol were blended with a highly water soluble polymer, polyvinyl pyrrolidone (PVP) and later electrospun into continuous uniform virus-blended PVP nanofibers. The resulting electrospun mats of virus-PVP nanofibers maintained their ability to infect bacterial hosts after being resuspended in a buffer solution.[13] Blending of two polymeric components has also been performed to achieve certain specific chain conformations in polymeric biomaterials. For instance, blending of regenerated silk with polyethylene oxide (PEO) was performed to avoid the development of insoluble and brittle β-sheets of silk fibroin.[14] Furthermore, blending of silk fibroin with a water soluble and biocompatible polymer, PEO, enhanced the utility of the resulting electrospun mats in *in vitro* and *in vivo* conditions. Another biomacromolecule, dextran, was blended with biodegradable poly(D,L-lactide-*co*-glycolide) (PLGA) to prepare electrospun membranes for biomedical applications.[15] Due to the high water solubility of dextran and PLGA, the water solubility of the resultant electrospun mats was controlled by a post-spinning UV crosslinking process that involved irradiation of the methacrylate-substituted dextran in the presence of a photoinitiator. In another study, PLGA was blended with biocompatible but hydrophobic poly(D, L-lactide) (PLA) to enhance the water solubility of the resulting electrospun scaffolds.[16]

A few aspects need to be considered when electrospinning is performed from blends of polymer solutions. For a blend of two polymers (in the same solvent or different solvents), the mixture should be homogenous so that the resultant mat possesses a uniform spatial composition. In addition to being thermodynamically miscible, the interactions between the polymer and the solvent of the opposing pair are of critical importance in a four-component system (dissolution of polymers in different solvents). Hence, the thermodynamic and kinetic aspects of *mixing* need to be considered when utilizing blends for electrospinning.

Another way to produce electrospun mats comprising of two polymeric components, whether miscible or immiscible, is to electrospin two polymers

simultaneously in a side-by-side fashion. Very recently, researchers have also been able to electrospin hollow silica[17] and ceramic[18] fibers by cospinning two solutions in a sheath-core fashion. As will be discussed later, in our approach the two polymer solutions do not come in physical contact until they reach the end of the spinneret where the process of fiber formation begins.

We have designed an electrospinning device where two polymer solutions have been electrospun simultaneously in a side-by-side fashion[19]. This allows having a bicomponent electrospun mat that possesses properties from each of the polymeric components. For instance, one of the polymers could contribute to the mechanical strength while the other could enhance the wettability of the resulting non-woven web. This could be useful for a protective clothing application. In fact by suitably choosing the constituent components based on their respective properties, the potential of these bicomponent fibers to be utilized in various applications becomes enhanced. These applications could include biomedical, protective, structural, sensing and so forth. The primary purpose of the present study, however, was to demonstrate the feasibility of this new methodology to produce submicron bicomponent fibers via electrospinning. As will be seen later, the strength of this methodology is to effectively electrospun immiscible and miscible polymer pairs to yield submicron bicomponent fibers.

In the following sections, the new bicomponent electrospinning device will be described. Preliminary results on poly(vinyl chloride)/segmented polyurethane (PVC/Estane®) and poly(vinyl chloride)/poly(vinylidiene fluoride) (PVC/PVDF) bicomponent fibers will be presented. It is important to note here that PVC/Estane® is a miscible system whereas PVC/PVDF is an immiscible system. PVC has a glass transition temperature of ca. 85 ^{o}C and is therefore a glassy and stiff material at room temperature. The mechanical properties of PVC, especially toughness can be enhanced by suitable plasticization.[20]. When blended with a thermoplastic urethane-based polymer, Estane®, it is expected that the resulting mechanical toughness would be improved depending on the composition ratio. PVDF on the other hand is semi-crystalline and also displays piezoelectric behavior.[21]. By incorporating a glassy and stiff polymer like PVC with PVDF, it is expected that the resulting system will possess characteristics of both the components. However, the choice of these specific systems was undertaken primarily to

identify the two components easily in each polymer pair by means of energy dispersive spectroscopy (EDS), thereby demonstrating the feasibility of electrospinning a bicomponent fiber. The EDS detector, which was a part of the scanning electron microscope (SEM) utilized in this study to investigate the morphology of the fibers, had a minimum resolution of 1μm x 1μm x 1μm. This allowed characterization the local composition of the bicomponent fibers at the micro level.

5.3 Experimental

5.3.1 Bicomponent Electrospinning Device

The schematic of the new device is shown in Figure 5.1, where the two plastic syringes each containing a polymer solution lie in a side-by-side fashion. A common syringe pump (K D Scientific, model 100) controlled the flow rate of the two polymer solutions. The platinum electrodes dipped in each of these solutions were connected in parallel to the high voltage DC supply (Spellman CZE 1000R). The free ends of the Teflon needles attached to the syringes were adhered together. The internal diameter of the Teflon needle was 0.7 mm with a wall thickness of ca. 0.2 mm and the length of the Teflon needles was ca. 6 cm. The grounded target used for collecting the solidified polymer filaments was a steel wire (diameter ~ 0.5mm) mesh of count 20x20 (20 steel wires per 1" each in the horizontal and vertical axes). It is also possible to use other kinds of substrates as well, e.g. the grounded target can be in the form of a cylindrical mesh that can be rotated to obtain filaments oriented in the extrusion direction. The fibers can also be collected on a wide array of substrates including wax paper, Teflon, thin polymer films and so forth. Choice of substrate can often facilitate easy collection and isolation of the fibers from the target.

5.3.2 Materials

PVC, weight average molecular weight, M_w, of 135,900 g/mol in the form of a fine powder, PVDF, weight average molecular weight, M_w, of 250,000 g/mol in the form of pellets and Estane® 5750, a polyether based segmented polyurethane supplied by Noveon Inc., also in the form of pellets was utilized for this study. Molecular weight data for Estane® 5750 could not be obtained, as the information was deemed proprietary. All the three polymers were dissolved separately in N,N-dimethylacetamide (DMAc) at different

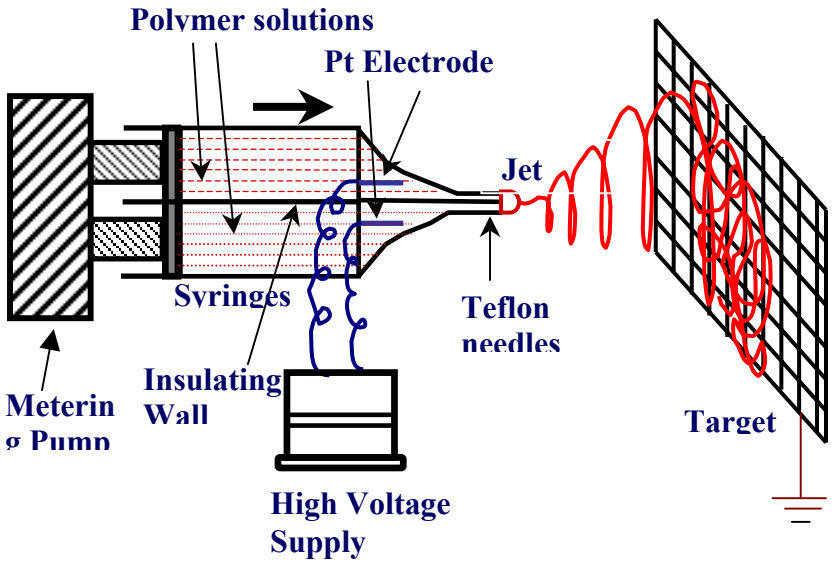

Figure 5.1 Schematic representation of the side-by-side bicomponent fiber electrospinning device.

weight concentrations ranging from 20-25-wt%. Polymer films were also cast from blends of PVC and Estane® in N,N-dimethylformamide (DMF) at different compositions (0, 25, 50, 75 and 100 wt% of Estane®). EDS was performed on solvent cast films of miscible PVC/Estane® blends to calibrate the peak intensities of oxygen (O) and chlorine (Cl) with the actual composition in the blend. Prior to SEM analysis all fiber and cast film samples were dried at 60 ^{o}C in vacuum for 8 h to eliminate any residual solvent. All solvents utilized in this study were purchased from Sigma Aldrich.

5.3.3 Measurements and Characterization

The viscosities of the polymer solutions were measured with an AR-1000 Rheometer, TA Instruments Inc. The measurement was done in the continuous ramp mode at room temperature (25 ^{o}C) using the cone and plate geometry. The sample was placed between the fixed Peltier plate and a rotating cone (diameter: 4 cm, vertex angle: 2^{o}) attached to the driving motor spindle. The changes in viscosity and shear stress with change in shear rate were measured. A computer interfaced to the rheometer recorded the resulting shear

stress vs. shear rate data. For the three solutions investigated in the present study, the shear stress vs. shear rate curve was linear within the range of shear rates investigated, thereby indicating Newtonian behavior. The slope of the linear shear stress-shear rate relationships gave the Newtonian or zero shear rate viscosities, η_o. The viscosity of the polymer solutions is of importance as it influences the final diameter of the electrospun fibers[22-24]. It is important to note, however, that the extensional viscosity of the jet while in flight to the target is undoubtedly very influential in governing the stretching induced in the jet. However, a thorough study of the effect of extensional viscosity on fiber formation in electrospinning has not been reported to date. For the present study, the zero shear rate viscosities are reported. The η_o of the polymer solutions were 8.7, 4.9 and 5.6 Pa·s respectively for PVC (25wt% in DMAc), Estane® (20wt% in DMAc) and PVDF (20wt% in DMAc) solutions.

An Oakton® conductivity tester, model TDStestr 20 was utilized to measure the conductivity of the polymer solutions. Prior to its use, the conductivity tester was calibrated by standard solutions procured from VWR Scientific®. The conductivities of the three polymer solutions were 7, 38 and 2 μS/cm respectively for PVC (25wt% in DMAc), Estane® (20wt% in DMAc) and PVDF (20wt% in DMAc).

A Leo® 1550 Field Emission Scanning Electron Microscope (FESEM) was utilized to visualize the morphology of the bicomponent polymer filaments. All the images were taken in the back-scattered mode, as the back-scattered detector is more sensitive to the electron density differences arising due to the presence of different chemical moieties, viz. Cl, O and F in PVC, Estane® and PVDF respectively. The samples were sputter-coated by a Cressington® 208HR to form a 5-10 nm conducting layer of Pt/Au layer on the surface of the fibers and films. This was done to reduce the charging of the non-conducting polymeric surfaces, when exposed to the electron beam in SEM. EDS in conjunction with SEM was utilized to investigate the morphology and local composition of the bicomponent fibers.

5.4 Results and Discussion

Single component electrospinning of varying % weight concentrations of PVC, PVDF and Estane® in DMAc was conducted to optimize the process conditions. The results are shown in Figure 5.2. The suitable process parameters at which uniform non-

beaded fibers were obtained are listed in Table 5.1. At these conditions, stable jets were formed and the fiber diameter of these filaments was in the range of 285 nm – 2 μm. The concentrations for PVC, PVDF and Estane® in DMAc were 25, 20 and 20 wt % respectively. These concentrations were utilized for electrospinning bicomponent systems as well. Table 5.2 provides the zero shear viscosity and the conductivity of these polymer solutions.

As shown in Figure 5.1, where the schematic of the bicomponent device is depicted, the two polymer solutions come in contact only at the tip of the Teflon needles. Even though the two polymer solutions are charged to the same polarity, some amount of mixing of the two components is expected to take place as the two solutions reach the end of the Teflon needle tips. Under stable electrospinning conditions, a fluctuating jet was observed for PVC/Estane® and PVC/PVDF at 14 and 15 kV respectively at a target distance of 20 cm and total flow rate of 3 ml/h. The corresponding average electric fields can be expressed as 0.7 kV/cm and 0.75 kV/cm respectively. Interestingly, when the distance between the Teflon needle-tips and the target was ca. 9 cm or larger, a single common Taylor cone was observed. From the surface of this Taylor cone, a fluctuating jet was ejected. The position of ejection of the jet on the surface of the Taylor cone changed very rapidly with time and led to a somewhat non-steady flow of the polymer solution. These fluctuations likely influence the extent of mixing of the two charged solutions when they come in contact at the tip of the Teflon needles. At distances larger than 25 cm, the jet was not continuous and the Taylor cone dripped due to weak field strength that did not convey the jet to the grounded target. At distances less than ca. 9 cm, two Taylor cones were observed to emanate from each of the two Teflon needles. As a result, two jets were observed to eject form each Taylor cone under these conditions. At such low distances (< 9 cm), the field strength was relatively strong, thereby inducing a strong electrostatic repulsion between the two polymer solutions emanating from each Teflon needle. This lead to the formation of two Taylor cones and subsequently two separate but identically charged (in terms of polarity) jets causing the formation of two zones of fiber collection on the target, each corresponding to only one of the two respective polymer components. For the systems investigated in this study, bicomponent electrospinning was conducted at a target distance of 10-25 cm from the needle tips.

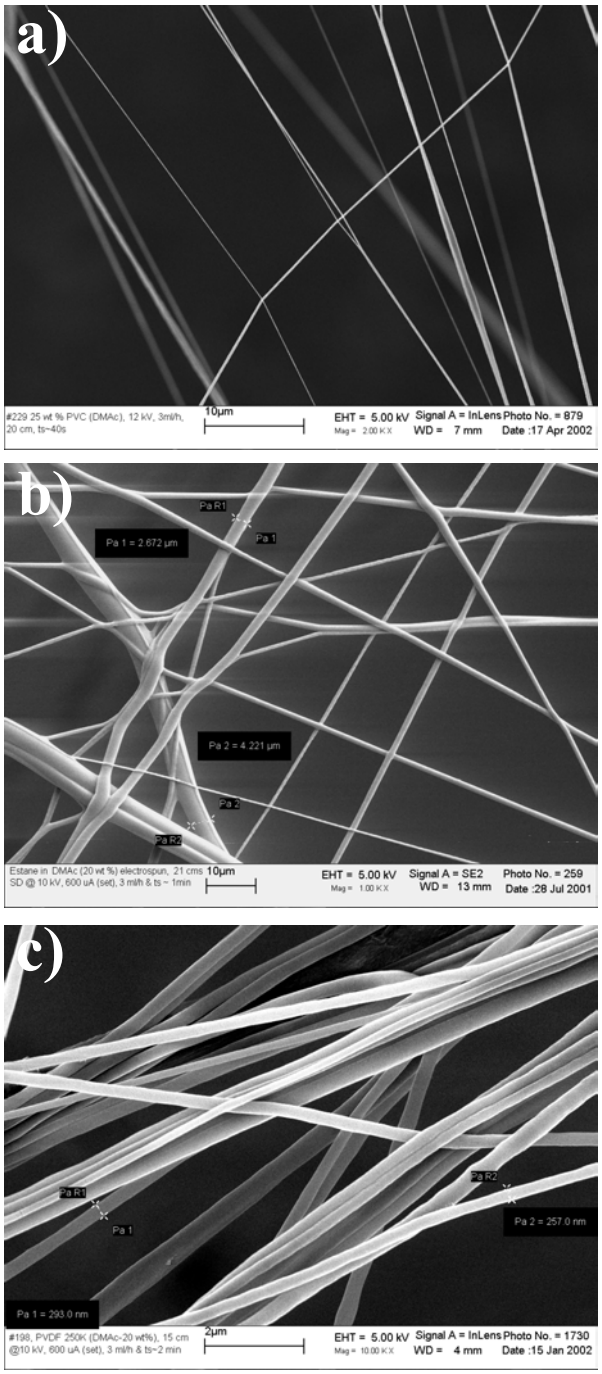

Figure 5.2 a) FESEM micrograph of PVC electrospun at 25 wt% (DMAc), 12 kV, 3ml/h & 20 cm. Fiber diameter ~ 170 – 400 nm b) FESEM micrograph of Estane® electrospun at 20 wt % (DMAc), 10 kV, 3 ml/h & 21 cm. Fiber diameter ~320 nm – 4 µm c) FESEM micrograph of PVDF electrospun at 20 wt% (DMAc), 10kV, 3ml/h & 15 cm. Fiber diameter ~ 230 – 625 nm.

Table 5.1 Optimized process parameters to electrospin single component PVC, Estane® and PVDF polymer systems and the resulting average fiber diameter.

Polymer system	% wt Conc. in DMAc to form non-beaded uniform fibers	Electric potential for stable jet formation (KV)	Distance between the spinneret and target (cm)	Flow rate (ml/h)	Average fiber diameter (nm)
PVC	25	12	20	3	285
Estane®	20	10	21	3	2160
PVDF	20	10	15	3	428

Table 5.2 Conductivity and zero shear rate viscosities of the three polymer solutions. All measurements were done at 25 ^{o}C.

Polymer system	Conductivity (μS/cm)	Zero shear rate viscosity (Pa·s)
PVC (25 wt% in DMAc)	**7**	**8.7**
Estane® (20 wt% in DMAc)	**38**	**4.9**
PVDF (20 wt% in DMAc)	**2**	**5.6**

Recall that under these conditions, a single Taylor cone and consequently a single jet was observed to form. The electrospinning conditions utilized for the miscible PVC/Estane® are summarized as: 14kV, 3ml/h, 15cm and 25wt% PVC with 20wt% Estane. For the immiscible PVC/PVDF, the conditions were: 15kV, 3ml/h, 20cm and 25wt% PVC with 20wt% PVDF. The back-scattered FESEM electron image of the dried PVC/Estane® electrospun web can be seen in Figure 5.3a. EDS was performed on several spatial positions within the mat, but of particular importance are the two regions marked as 'A' and 'B'. Region 'A' exhibited an intense peak of chlorine (Cl), indicating the local composition to be principally comprised of PVC (Figure 5.3b), whereas, region 'B' exhibited an intense peak of oxygen (O), indicating the local dominance of Estane® (Figure 5.3c). It is important to note the presence of a smaller peak corresponding to

oxygen in Figure 5.3a. This peak was relatively weak but it does indicate the presence of Estane® in the predominantly PVC rich fiber at region 'A'. In Figure 5.4a, the back-scattered SEM on bicomponent PVC/PVDF electrospun web is shown. Similar to what was described above, EDS was performed on several spatial positions within the electrospun mat, but of particular importance are the two regions marked as 'A' and 'B'. Region 'A' (Figure 5.4b) was observed to be predominantly composed of PVC, as indicated by a strong peak of chlorine in Figure 5.4b, whereas region 'B' was primarily composed of PVDF, as indicated by the strong peak of fluorine in Figure 5.4c. It is important to note that smaller peaks corresponding to trace amounts of fluorine and chlorine respectively can be observed as well in Figures 5.4b and 5.4c. In both the cases, it can be concluded that although fibers composed primarily of either component were observed to form, the presence of trace amounts of the other component indicates some level of physical mixing in the two solutions. To obtain a better understanding of this phenomenon, EDS was performed along the length of a given fiber to study the changes in local composition, if any. Bicomponent fibers chosen for these investigations were typically a micron or so in diameter as the minimum resolution of the EDS detector was 1μm x 1μm x 1μm. In fact, the diameter for these bicomponent fibers of PVC/Estane® and PVC/PVDF ranged from 100nm to a few microns.

When EDS was conducted on different regions along a 15 μm length of a 'PVC-rich' fiber in the PVC/Estane® mat, it was found that the ratio of the peak intensity corresponding to chlorine to that of oxygen varied from 4.6 to 7.7 (Figure 5.5a). Similar measurements performed on regions along a 25 μm length of a 'PVDF-rich' fiber in the PVC/PVDF mat, indicated that the ratio of the peak intensity corresponding to fluorine with that of chlorine varied from 1.8 to 2.5 (Figure 5.5b). These results indicated that even though fibers comprised predominantly of either component were observed, the relative amount of a given component varied significantly along the length of the fiber. Restated, the mixing of the two components changes with time within the time frame of electrospinning process that promotes variations in the composition along the length of the fiber. These variations in the composition of the bicomponent fibers are attributed to

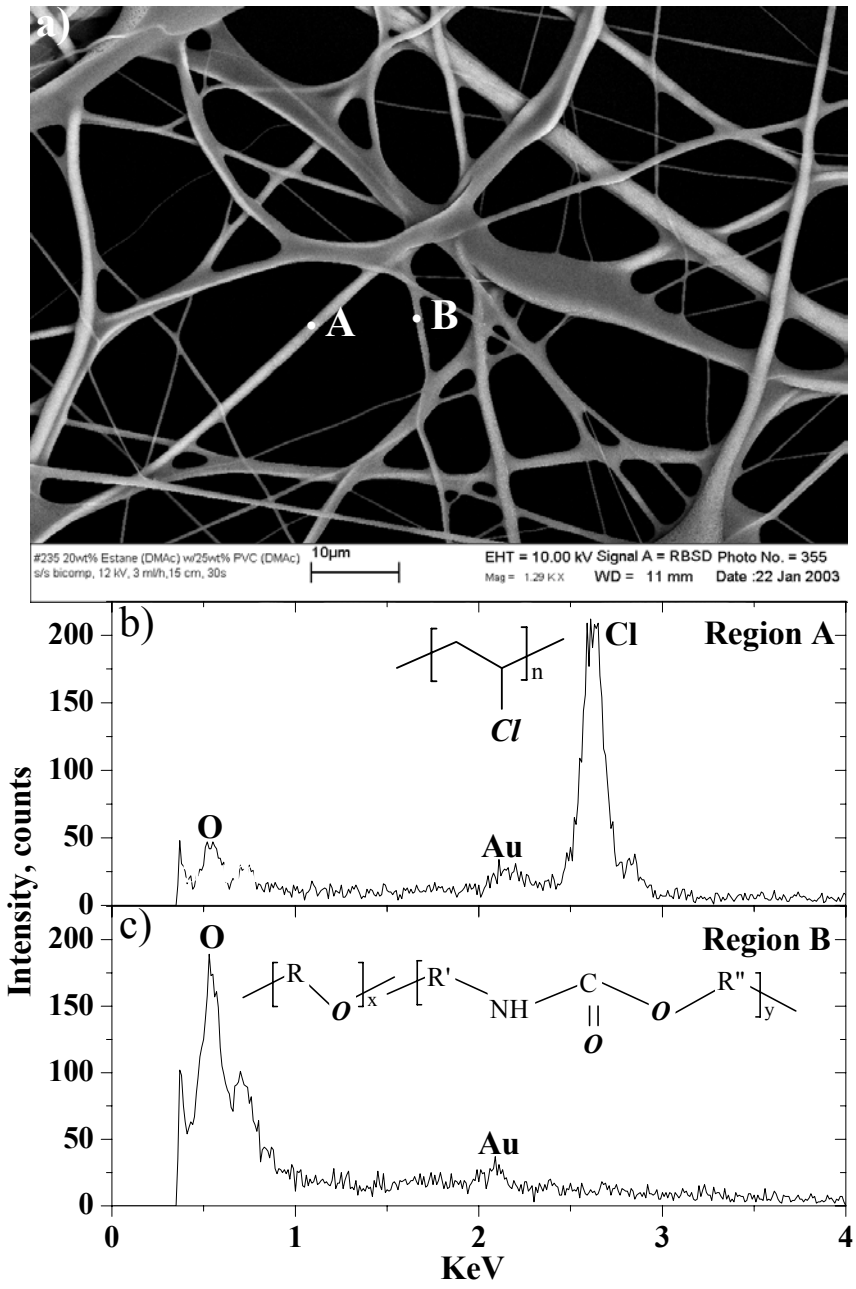

Figure 5.3 a) SEM of PVC/Estane® electrospun mat. EDS results conducted on regions 'A' and 'B' indicate the local composition of the fibers in b) and c) respectively. The chemical structures of PVC and Estane® are shown along the intense peaks arising due to chlorine (Cl) and oxygen.

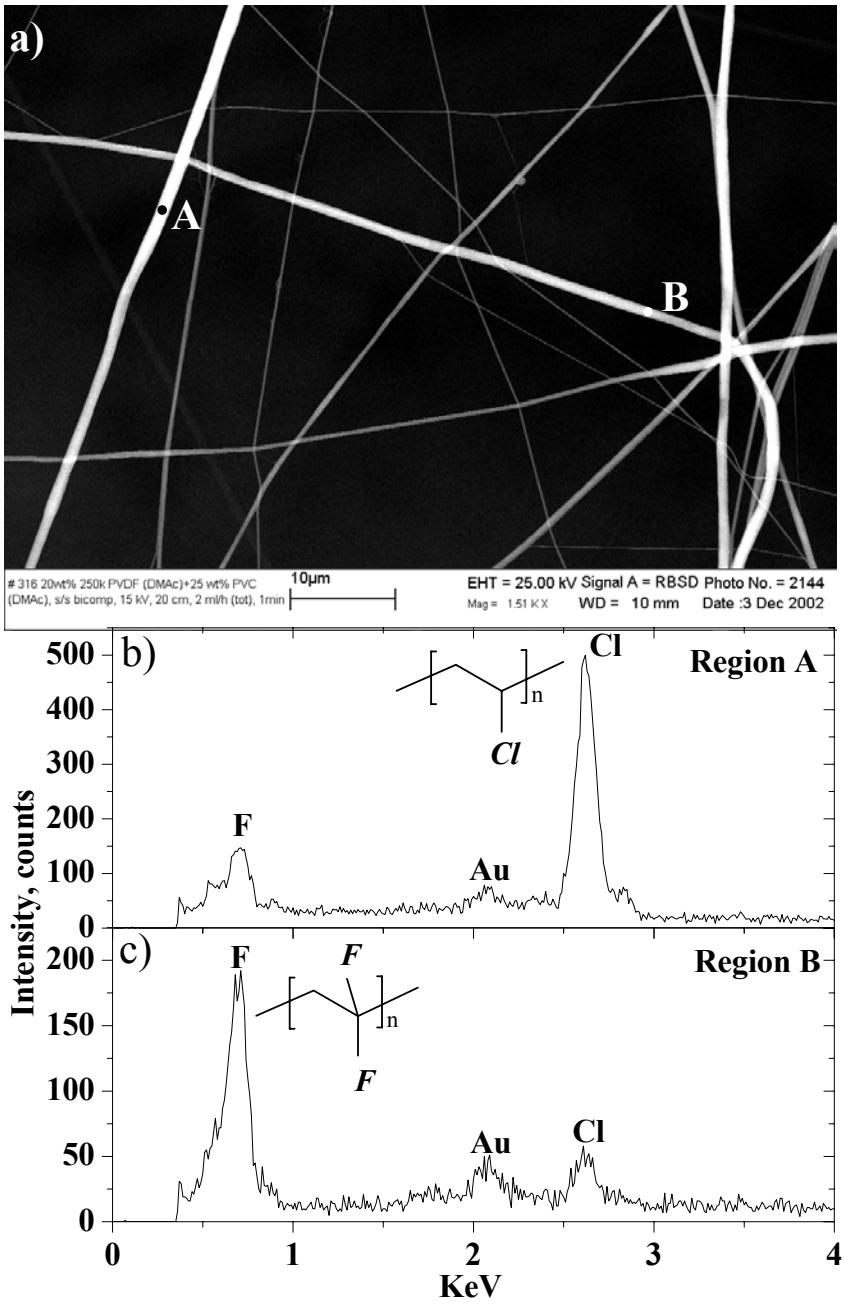

Figure 5.4 a) SEM of PVC/PVDF electrospun mat. EDS results conducted on regions 'A' and 'B' indicate the local composition of the fibers in b) and c) respectively. The chemical structures of PVC and PVDF are shown along the intense peaks arising due to chlorine (Cl) and fluorine.

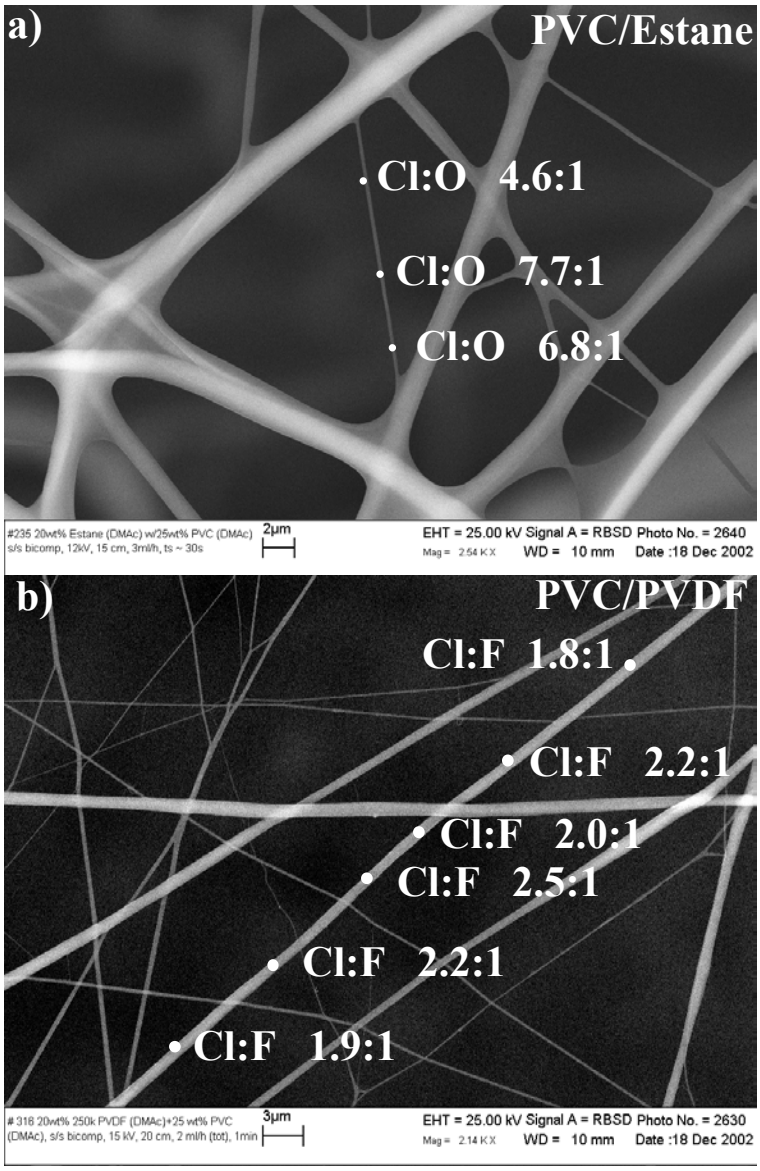

Figure 5.5. Variation in the peak intensity ratio of a) chlorine (Cl) and oxygen (O) in bicomponent PVC/Estane and b) chlorine (Cl) and fluorine (F) in bicomponent PVC/PVDF electrospun webs.

the fluctuations of the common jet on the surface of the Taylor cone. Chain diffusion and relaxation can also enhance the mixing of the two components. It is useful to consider that both the jets emanating from the Teflon needle tips carry the same electrostatic

charge and therefore experience mutual electrostatic repulsion. This is expected to hinder the mixing of the two solutions to some degree. In addition, PVC can develop a low degree of crystallinity while PVDF distinctly crystallizes to a higher extent when solidified from solution. Hence, the amount of crystallinity induced in these fibers as the solvent evaporates during the flight of the fibers to the grounded target will also influence the extent of mixing of the two components. Therefore the mixing of the two charged solutions in bicomponent electrospinning is a competing phenomena between several effects - the fluctuations on the jet, electrostatic repulsion between the like-charged jets, diffusion of polymeric chains of one component in the other, chain relaxation, evaporation rate of the solvent and solvent induced crystallization in semi-crystalline polymers.

To estimate the composition of the PVC/Estane® bicomponent fibers in terms of actual wt% of either component, EDS analysis was conducted on solvent cast (non-spun) films of miscible PVC/Estane®. The peak intensity ratios of Cl to O as observed by EDS in these films of miscible PVC/Estane® were calibrated to the actual wt% of Estane®. Five films of PVC/Estane® were solvent cast from DMF at 0, 25, 50, 75 and 100 wt% of Estane® that were ca. 125 μm in thickness. As mentioned previously, prior to SEM these films were oven dried in vacuum at 60 ^{o}C for 8 h to eliminate any residual solvent. SEM results indicated uniform surface morphology, as expected. EDS analysis was performed on each film at different spatial positions to ascertain the local composition. The average peak intensities of Cl and O were plotted after correcting for the background in Figure 5.6a. It can be seen that the corrected peak intensities of Cl and O decrease and increase linearly with wt% of Estane® respectively. The ratio of corrected peak intensities of Cl to O was plotted as a function of wt% of Estane® and is shown in Figure 5.6b. The four data points (at 0 wt% Estane®, the Cl:O approaches infinity, and is thus not plotted) can be fitted empirically to a good approximation as an exponential decay. It is noted that the curve fitting of the data points to an exponential decay does notbear any particular physical significance. Recall that the ratio of peak intensity of Cl:O in the PVC/Estane® bicomponent fiber varied from 4.6 to 7.7 along its length. These correspond to a variation in wt% Estane® from 35 to 27 respectively. A similar exercise could not be performed on

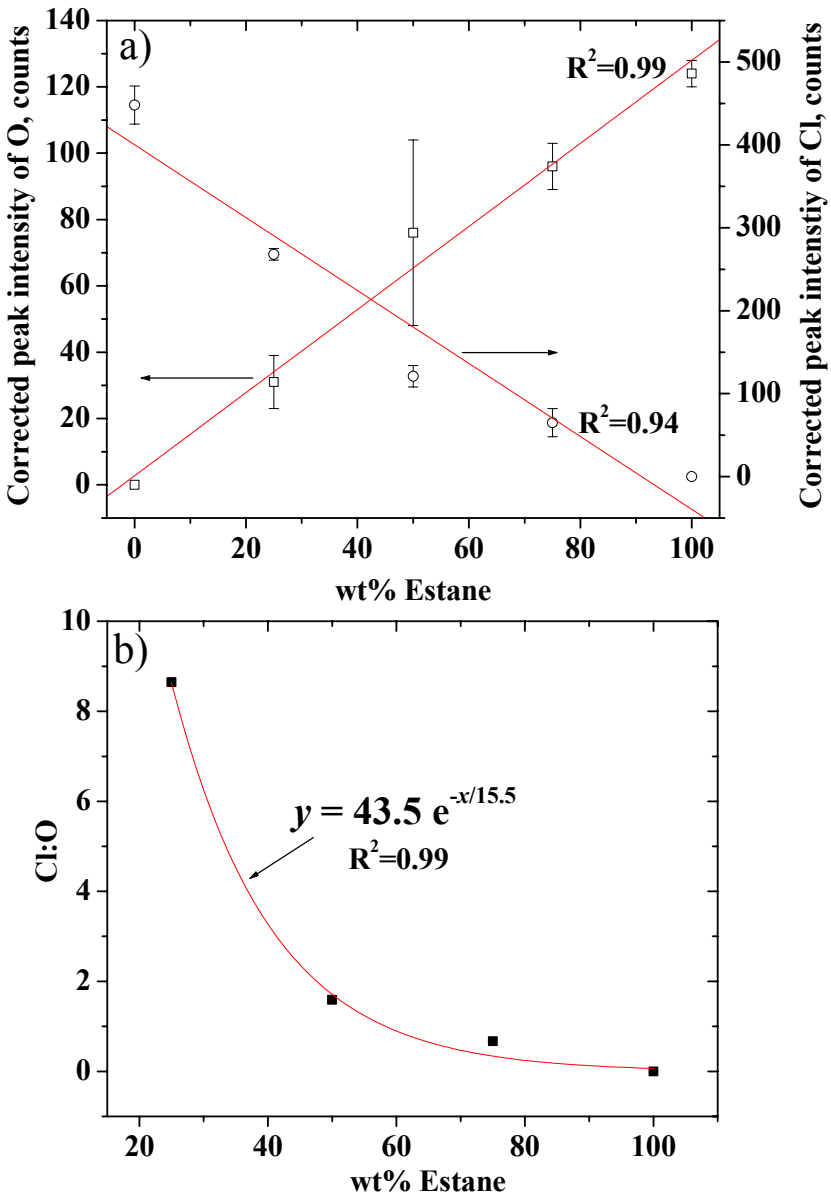

Figure 5.6 a) Linear variation of peak intensity of O and Cl and b) variation of the ratio of the average peak intensities of Cl and O as a function of composition in the solvent cast blend films of PVC/Estane®. The data in b) is fitted to an exponential decay, as indicated.

PVC/PVDF as phase separation occurred in the solvent cast films from its blends due to their immiscibility.

5.5 Conclusions

Two polymer solutions were electrospun simultaneously in a side-by-side fashion to produce bicomponent fibers that had diameters in the range of 100 nm to a few

microns. A miscible, PVC/Estane®, and an immiscible, PVC/PVDF were electrospun in this fashion. For each of the pairs investigated, PVC/Estane® and PVC/PVDF, EDS was utilized to identify the respective components by detecting the signal corresponding to chlorine, oxygen and fluorine from PVC, Estane® and PVDF respectively. It was found that the ratio of the peak intensities of Cl and O in PVC/Estane® and Cl and F in PVC/PVDF varied along the length of the fibers, viz. 4.6 to 7.7 for Cl:O in PVC/Estane® and 1.8 to 2.5 for Cl:F in PVC/PVDF. The ratio of the peak intensities corresponding to Cl and O in the miscible PVC/Estane® was calibrated to the actual wt% of Estane® (35 to 27 wt% respectively). Utilizing the methodology described in this study, the feasibility of electrospinning a bicomponent fiber has been demonstrated.

Acknowledgements

This material is based upon work supported by, or in part by, the U.S. Army Research Laboratory and the U.S. Army Research Office under grant number DAAD19-02-1-0275 Macromolecular Architecture for Performance (MAP) MURI. The authors thanks Prof. Chip Frazier, Wood Science Department, Virginia Tech, for allowing the use of AR-1000 Rheometer for viscosity measurements.

References

(1) Doshi J; Reneker, D. H. *Journal of Electrostatics* **1995**, *35*, 151-160.

(2) Fong, H.; Chun, I.; Reneker, D. H. *Polymer* **1999**, *40*, 4585-4592.

(3) Kim, J.-S.; Reneker, D. H. *Polymer Engineering and Science* **1999**, *39*, 849-854.

(4) Deitzel, J. M.; Kleinmeyer, J. D.; Hirvonen, J. K.; Beck, T. N. C. *Polymer* **2001**, *42*, 8163-8170.

(5) Srinivasan, G.; Reneker, D. H. *Polymer International* **1995**, *36*, 195-201.

(6) Doshi, J.; Reneker, D. H. *Journal of Electrostatics* **1995**, *35*, 151-160.

(7) Fong, H., 1999; p 109 pp.

(8) Deitzel, J. M.; Kleinmeyer, J. D.; Hirvonen, J. K.; Beck Tan, N. C. *Polymer* **2001**, *42*, 8163-8170.

(9) Srinivasan, G.; Reneker, D. H. *Polymer International* **1995**, *36*, 195-201.

(10) Demir, M. M.; Yilgor, I.; Yilgor, E.; Erman, B. *Polymer* **2002**, *43*, 3303-3309.

(11) Pinto, N. J.; Johnson, A. T., Jr.; MacDiarmid, A. G.; Mueller, C. H.; Theofylaktos, N.; Robinson, D. C.; Miranda, F. A. *Applied Physics Letters* **2003**, *83*, 4244-4246.

(12) Kahol, P. K.; Pinto, N. J. *Synthetic Metals* **2004**, *140*, 269-272.

(13) Lee, S.-W.; Belcher, A. M. *Nano Letters* **2004**, *4*, 387-390.

(14) Jin, H.-J.; Fridrikh, S. V.; Rutledge, G. C.; Kaplan, D. L. *Biomacromolecules* **2002**, *3*, 1233-1239.

(15) Jiang, H.; Fang, D.; Hsiao, B. S.; Chu, B.; Chen, W. *Biomacromolecules* **2004**, *5*, 326-333.

(16) Kim, K.; Yu, M.; Zong, X.; Chiu, J.; Fang, D.; Seo, Y.-S.; Hsiao, B. S.; Chu, B.; Hadjiargyrou, M. *Biomaterials* **2003**, *24*, 4977-4985.

(17) Loscertales, I., G.; Barrero, A.; Márquez, M.; Spretz, R.; Velarde-Ortiz, R.; Larsen, G. *Journal of the American Chemical Society* **2004**, *126*, 5376-5377.

(18) Li, D.; Xia, Y. *Nano Letters* **2004**, ACS ASAP.

(19) Gupta, P.; Wilkes, G. L. *Polymer* **2003**, *44*, 6353-6359.

(20) Cano, J. M.; Marin, M. L.; Sanchez, A.; Hernandis, V. *Journal of Chromatography, A* **2002**, *963*, 401-409.

(21) In'acio, P.; Marat-Mendes, J. N.; Dias, C. J. *Ferroelectrics* **2003**, *293*, 351-356.

(22) McKee, M. G.; Wilkes, G. L.; Colby, R. H.; Long, T. E. *Macromolecules* **2004**, *37*, 1760-1767.

(23) Yarin, A. L.; Koombhongse, S.; Reneker, D. H. *Journal of Applied Physics* **2001**, *90*, 4836-4846.

(24) Buer, A.; Ugbolue, S. C.; Warner, S. B. *Textile Research Journal* **2001**, *71*, 323-328.